JOURNAL OF Applied Polymer SCIENCE

Thermal Properties and Flame-Retardancy of Ethylene-Octene Copolymer/Organ-Montmorillonite Nanocomposites

Shuhao Qin,[1] Qingfeng Li,[1,2] Jie Yu,[1] Liangqing Wei,[1] Jianbing Guo,[1] Huiju Shao,[1] Shan Liang,[1,2] Zhu Luo[2]

[1]National Engineering Research Center for Compounding and Modification of Polymeric Materials, Guizhou, Guiyang 550014, China

[2]College of Material and Metallurgy of Guizhou University, Guizhou, Guiyang 550025, China

Correspondence to: J. Yu (E-mail: yujiegz@126.com)

ABSTRACT: Two series of thermoplastic elastomer ethylene-octene copolymer (POE) composites and maleated ethylene-octene (POE-*g*-MAH) with organo-montmorillonite (OMMT) were prepared via melting processing to study their thermal properties and flame-retardancy. The morphology was studied by transmission electron microscope (TEM). The influence of clay dispersion on thermal and flammability properties was investigated by using thermal gravimetric analysis (TGA) and cone calorimeter. TEM showed that agglomerated structure of OMMT within POE matrix but intercalated/exfoliated structures throughout POE-*g*-MAH matrix. The different dispersion of OMMT resulted in more significant improvements on thermal stability and flame-retardancy in the POE-*g*-MAH/OMMT nanocomposites compared with POE/OMMT microcomposites. © 2012 Wiley Periodicals, Inc. J. Appl. Polym. Sci. 000: 000–000, 2012

KEYWORDS: ethylene-octene copolymer; organo-montmorillonite; nanocomposites; thermal stability; flame-retardancy

Received 29 November 2011; accepted 6 March 2012; published online 00 Month 2012
DOI: 10.1002/app.37650

INTRODUCTION

Polymer/clay nanocomposites have been attracted the interests of academics and industries in the past several decades because of their improved mechanical, thermal, flammability, ablation resistance, and enhanced barrier properties.[1] One property of nanocomposites that has emerged as a particularly unique one is the improvement in flammability.[2] Montmorillonite, a 2 : 1 layered smectite clay, has a natural platy structure with individual platelets having thicknesses of 1 nm and lengths of the order of 100–1000 nm, has been widely used as renforcement materials for polymers because of their nanoscale size and intercalation properties.[3]

Blumstein (1965) first reported the improved thermal stability of a polymer/lay nanocomposite that is combined polymethylmethacrylate (PMMA) and montmorillonite clay. Although this clay-rich nanocomposite would undoubtedly reflect properties dominated by the inorganic phase, the indications of enhanced polymer thermal properties are clear.[4] The cone calorimetry is one of the most effective bench scale methods for studying the flammability properties of materials products.[5] Polymer/clay nanocomposites have been rendered even more attractive by recent demonstrations of their flame-retardant properties, namely, diminution of the heat release rate (HRR) peak, formation of protective char, and decrease in the rate of mass loss during combustion in the cone calorimeter test.[6] Gilman et al. reported that the presence of nanodispersed montmorillonite (MMT) clay in polymeric matrices produces a substantial improvement in fire performance.[4,7] Depending on the polymer, the peak HRR can be decreased between 50% and 70% in a cone calorimeter experiment. For example, the peak HRR of polyamide-6 (PA-6)/clay nanocomposites is decreased by 63% compared with virgin PA-6 at an external heat flux of 35 kW/m^2.[8] The general view of the flame retardant mechanism is that a high-performance carbonaceous silicate char builds up on the surface during burning; this insulates the underlying material and slows the mass loss rate (MLR) of decomposition products. However, this effect is negligible when the organoclay is not dispersed at the nanoscale level indicating that to obtain an effective surface layer, it is necessary to have a chemical interaction between the polymer matrix and the clay layer surface.[9] Ethylene-octene copolymer (POE) is a new family of polyolefin elastomer, which is developed using a metallocene catalyst by Dow and Exxon has received much attention due to its unique uniform distribution of comonomer content and narrow molecular weight distribution. These elastomers have been widely used as

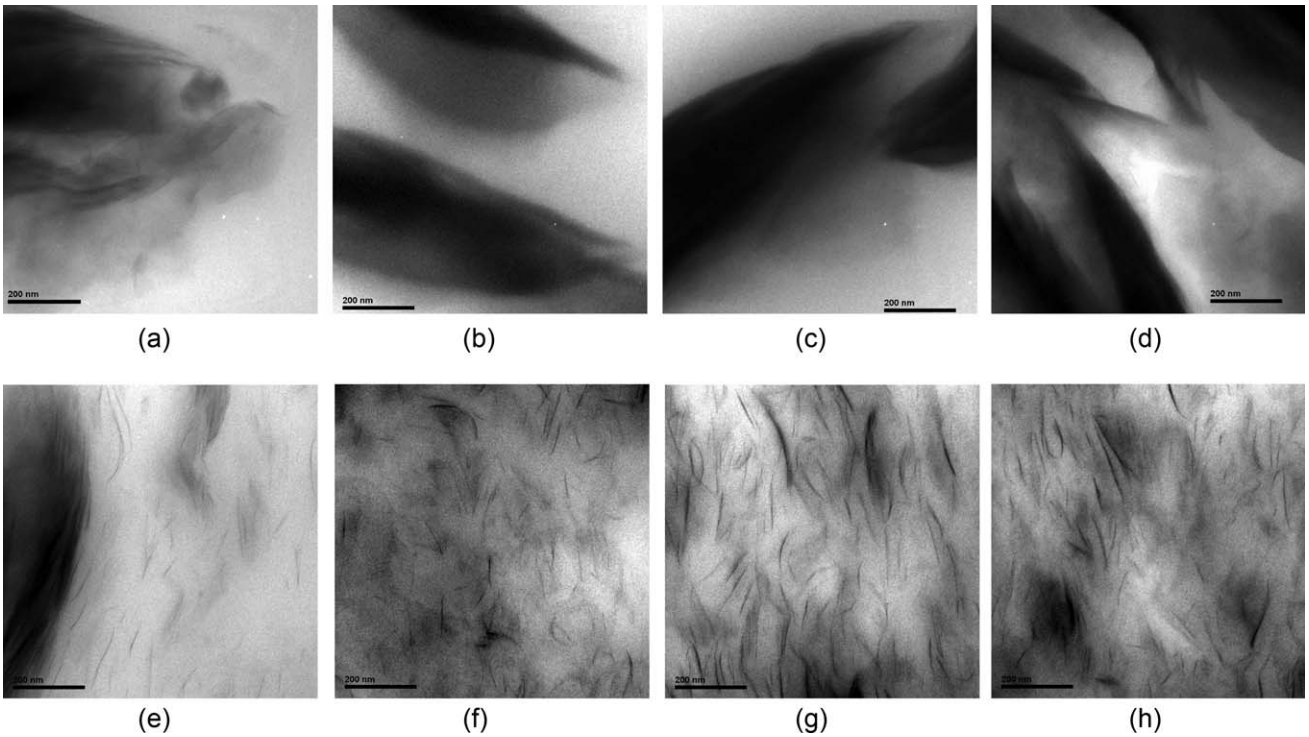

Figure 1. TEM microphotographs of composites; (a) POE with 5 wt % of OMMT, (b) POE with 15 wt % of OMMT, (c) POE with 25 wt % of OMMT, (d) POE with 35 wt % of OMMT, (e) POE-*g*-MAH with 5 wt % of OMMT, (f) POE-*g*-MAH with 15 wt % of OMMT, (g) POE-*g*-MAH with 25 wt % of OMMT, and (h) POE-*g*-MAH with 35 wt % of OMMT.

the main polymer or a value enhancing ingredient in compound formulations. Because POE does not include any polar groups in its backbone, it is thought that homogeneous dispersion of the hydrophilic clay minerals in the hydrophobic POE matrix is not realized. To obtain good dispersion of the organically modified clay in nonpolar POE, introduction of polymer functionalized with maleic anhydride or hydroxyl groups as compatibilizer has been proved as a successful way to facilitate interactions between these two dissimilar components.[1,5,10,11]

However, it seems that studies on thermal properties and flame-retardancy of POE/clay nanocomposites using the melt exfoliation method are rare in our literature survey. In this article, thermoplastic elastomer POE and maleated ethylene-octene (POE-*g*-MAH) with organo-montmorillonite (OMMT) were synthesized using melting processing to study their thermal properties and flame-retardancy, and the influence of OMMT dispersion on the thermal stability and flame-retardancy was discussed.

EXPERIMENTAL

Materials

The ethylene-octene elastomer (POE, Engage 8842, 45% octene, $M_w = 118{,}476$ and $M_n = 25{,}868$) was supplied by Dupont-Dow Chemicals. POE-*g*-MAH ($M_w = 112{,}921$ and $M_n = 24{,}758$, 45% octene) with a grafting degree of 0.6% was prepared by melt extrusion process. The OMMT prepared form pristine Na^+-MMT by ion exchange reaction using alkyl methyl dimethoxy ammonium chloride was provided by ZheJiang Fenghong Clay Chemicals Co (AnjI county seat, ZheJiang province, China).

Preparation of Composites

OMMT was dried before use for 12 h at 80°C in a vacuum oven to remove any moisture. POE and POE-*g*-MAH were dried for 12 h at 50°C before use. POE/OMT (0 wt %, 5 wt %, 15 wt %, 25 wt %, 35 wt %) and POE-*g*-MAH/OMT (0 wt %, 5 wt %, 15 wt %, 25 wt %, 35 wt %) composites were prepared in a two-screw extruder (TSE-35A/400-44-22, $L/D = 35$, $D = 35$ mm, Coperion Keya Machinery, Nanjing, China) at 140–210°C. The extrudates were pelletized and dried at 60°C for 24 h. The dried granules were compounded on a two-roll mill (Type SK-100, Shanghai Kechuang Rubber Plastic Mechanical Equipment, Shanghai, China) at 100°C for 3 min. The resulting composites were compression molded at 90°C for 5 min into standard samples.

TEM

The morphology was examined by transmission electron microscope (TEM) using a JEM 200CX (JEOL, Japan) TEM operating at an accelerating voltage of 120 KV. Ultrathin sections (60–80 nm) were cut from Izod bars perpendicular to the flow direction under cryogenic conditions using a LKB-5 microtome (LKB Co, Switzerland).

TGA

The thermal properties of the composites were studied on thermal gravimetric analysis (TGA) (TA, Q-50 instruments, New Castle, Delaware State) under 60 ml/min of compressed air and 40 ml/min flow of high purity grade nitrogen. About 8 mg of each of the sample was loaded in a ceramic sample pan and

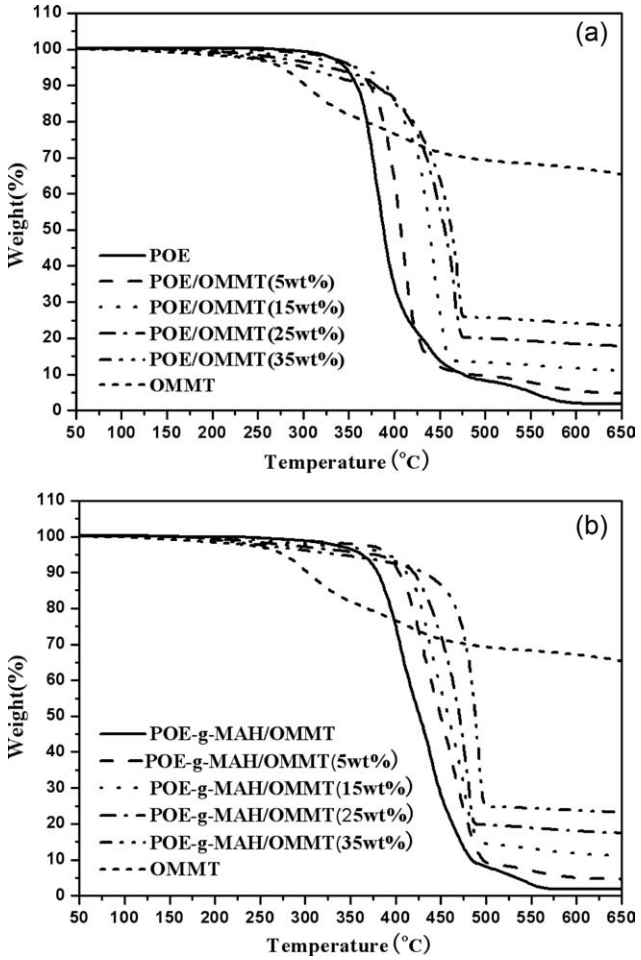

Figure 2. TGA curves for POE/OMMT (a) and POE-*g*-MAH/OMMT (b) composites.

heated from room temperature to 650°C at a heating rate of 20°C/min.

Cone Calorimeter

Flammability property of the samples (100 mm × 100 mm × 6 mm) was performed with an FTT, UK device according to ISO 5660 under a heat flux of 50 kW/m^2 at 20 ± 2°C and relative humidity 50 ± 5%. The cone calorimeter value is the average of three measurements and the results are considered reproducible to ±10%.

RESULTS AND DISCUSSION

Transmission Electron Microscopy

The TEM micrographs of POE/OMMT and POE-*g*-MAH/OMMT composites prepared with different content of OMMT are shown in Figure 1. The dark lines represent each OMMT layers and the white background corresponds to the polymer matrix. In Figure 1(a–d), the OMMT layers consist of oriented multilayered stacks, neither intercalation of the POE chains nor exfoliation of the silicate platelets are achieved, forming microcomposites. On the other hand, in the micrographs of POE-g-MAH/OMT nanocomposites, better dispersion of OMT in POE-g-MAH resin was obtained and many disordered single platelets can be seen, which indicates that a mixed intercalated/delaminated structure was formed showed in Figure 1(e–h).

The nonpolar POE lacks of favorable interactions with OMT, which limits the dispersion of OMT in POE during melt compounding. The polar character of MAH grafted on POE-*g*-MAH results in favorable interaction and thus a special affinity for the silicate surfaces. The strong hydrogen bonding between MAH groups of POE-*g*-MAH and the oxygen atoms of silicates leads to the increase of the interlayer spacing of the clay and the weakening of the interactions between the layers.[12]

Thermal Stability

Thermal stability is an important property for which the composites morphology played an important role.[13] Clay layers have good barrier action, which can improve the thermal stability of polymer/clay nanocomposites. However, the dimethoxy ammonium chloride cation in the organoclay could suffer decomposition following the Hofmann elimination reaction, and its product would catalyze the degradation of polymer matrixes. Third, the clay itself can also catalyze the degradation of polymer matrixes. The latter two actions would reduce the thermal stability of polymer/clay nanocomposites. In summary, the OMMT has two opposing functions in the thermal stability of the polymer/clay composite, one is barrier effect which could improve the thermal stability, and the other is the catalysis effect toward the degradation of the matrix that would decrease the thermal stability. When adding a low fraction to the matrix, the clay barrier effect is predominant but with increasing loading, the catalyzing effect rapidly rises and becomes dominant, so that the thermal stability of the composites decreases layers.[14–19]

The thermal stability of OMMT, POE/OMMT, and POE-*g*-MAH/OMMT composites are tested by TGA, and their TGA curves, and data were shown in Figure 2 and Table I. The onset temperature occurs at 5% weight loss ($T_{5\%}$). In this article, $\triangle T_{5\%}$ is the temperature difference between POE/OMMT, POE-*g*-MAH/OMMT composites, and their matrix, respectively; for example, the +8.73 is the temperature difference between POE/OMMT (5 wt %) and POE matrix and the +28.12 is the temperature difference between POE-*g*-MAH/OMMT (5 wt %) and POE-*g*-MAH matrix. The "+" indicates that the $T_{5\%}$ temperature of composite is higher than that of its matrix and "−" indicates lower than that of its matrix.

As for POE/OMMT microcomposites, we can see that the $T_{5\%}$ temperatures of POE/OMMT (5 wt %) and POE/OMMT (15 wt %) are higher compared with POE matrix, which can be

Table I. TGA Data of the Two Series of Composites

	POE/OMMT		POE-*g*-MAH/OMMT	
OMMT (wt %)	$T_{5\%}$ (°C)	$\triangle T_{5\%}$ (°C)	$T_{5\%}$ (°C)	$\triangle T_{5\%}$ (°C)
0	346.27	0	362.91	0
5	355.2	+8.73	391.03	+28.12
15	358.69	+12.42	391.52	+28.61
25	327.68	−18.59	375.70	+12.79
35	300.20	−46.07	337.30	−25.61

Table II. Cone Calorimeter Test Data of POE/OMMT and POE-g-MAHH/OMMT Composites

	TTI (s)		Residue yield (% ± 0.5)		PHRR (kW/m^2)		Mean HRR (kW/m^2)	
OMMT (wt %)	POE/ OMMT	POE-*g*-MAH/ OMMT	POE/ OMMT	POE-*g*-MAH/ OMMT	POE/ OMMT	POE-*g*-MAH/ OMMT	POE/ OMMT	POE-*g*-MAH/ OMMT
0	43	40	0	0	1374	1571	430	521
5	29	35	5.3	7.3	938	594	391	335
15	24	30	14.7	15.4	597	437	291	234
25	22	32	20.5	22	478	334	218	178
35	21	35	25.2	27.7	378	315	204	149

attributed to the predominant barrier effect. The $T_{5\%}$ temperatures of POE/OMMT (25 wt %) and POE/OMMT (35 wt %) are lower compared with POE matrix because of the Hofmann elimination reaction. Comparing with POE-*g*-MAH matrix, POE-*g*-MAH/OMMT (5 wt %), POE-*g*-MAH/OMMT (15 wt %), and POE-*g*-MAH /OMMT (25 wt %) have higher $T_{5\%}$ temperatures where the barrier effect is predominant. The $T_{5\%}$ temperature of POE-*g*-MAH/OMMT (35 wt %) is lower than that of POE-*g*-MAH matrix where the catalyzing effect becomes dominant. For both series of composites, the thermal stability is improved with the low fraction of OMMT and deteriorated with high fraction. Whether or no, $\triangle T_{5\%}$ of POE-*g*-MAH/OMMT is always bigger than that of POE/OMMT at the same content of OMMT.

From the analysis above, we can come to the conclusion that the POE-*g*-MAH/OMMT nanocomposites have better thermal stability than POE/OMMT microcomposites and the better thermal stability is not due to the higher thermal stability of POE-*g*-MAH matrix but because of the strong effect of the better dispersion of OMMT. The well-exfoliated layers account for the improvement in thermal degradation resistance. The lower improvement on thermal degradation for POE/OMMT microcomposites is due to the agglomeration of OMMT.

Flammability Properties

The cone calorimeter is one of the most effective bench scale methods for investigating the combustion properties of polymer materials, which can be conveniently used to measure not only HRR but also many other flammability properties during burning,[13,20] including time to ignition (TTI), peak HRR (pHRR), MLR, effective heat combustion (EHC), specific extinction area (SEA), smoke production rate (SPR), and CO yield. Cone calorimeter revealed improved flammability properties for many types of clay-filled polymer nanocomposites. HRR, in particular pHRR was found to be the most important parameter to evaluate fire safety.[4,9,13] The cone calorimeter data reported here are averages of three replicated experiments.

TTI

TTI is given in Table II. The results show that TTI for both series of composites are shorter compared with their matrix, respectively, which could be ascribed to the low thermal stability of octadecyl trimethyl ammonium cation contained in the organoclay layers. Another reason is that the layers of OMMT cut off the heat at the surface of the composites to the substrate, making the heat assemble at the surface of samples and faster to ignition.[18] The third reason is related to the thermal stability of the composites.[6] The TTI of POE-*g*-MAH/OMMT nanocomposites is longer than that of POE-*g*-MAH/OMMT microcomposite at the same content of OMMT as a result of the higher thermal stability of the POE-*g*-MAH/OMMT nanocomposites.

HRR

Cone calorimeter reveals improved flammability properties for many types of polymer/clay nanocomposites. The HRR, in particular pHRR was found to be the most important parameter to evaluate fire safety.[5,13,21] Plots of the HRR for the composites

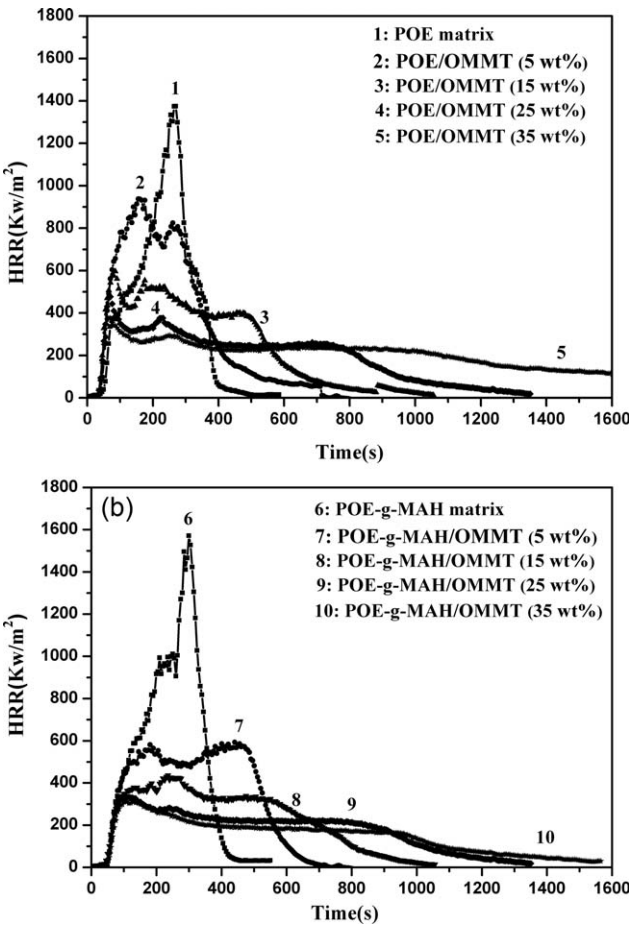

Figure 3. HRR plots of POE/OMMT (a) and POE-*g*-MAH/OMMT (b) composites.

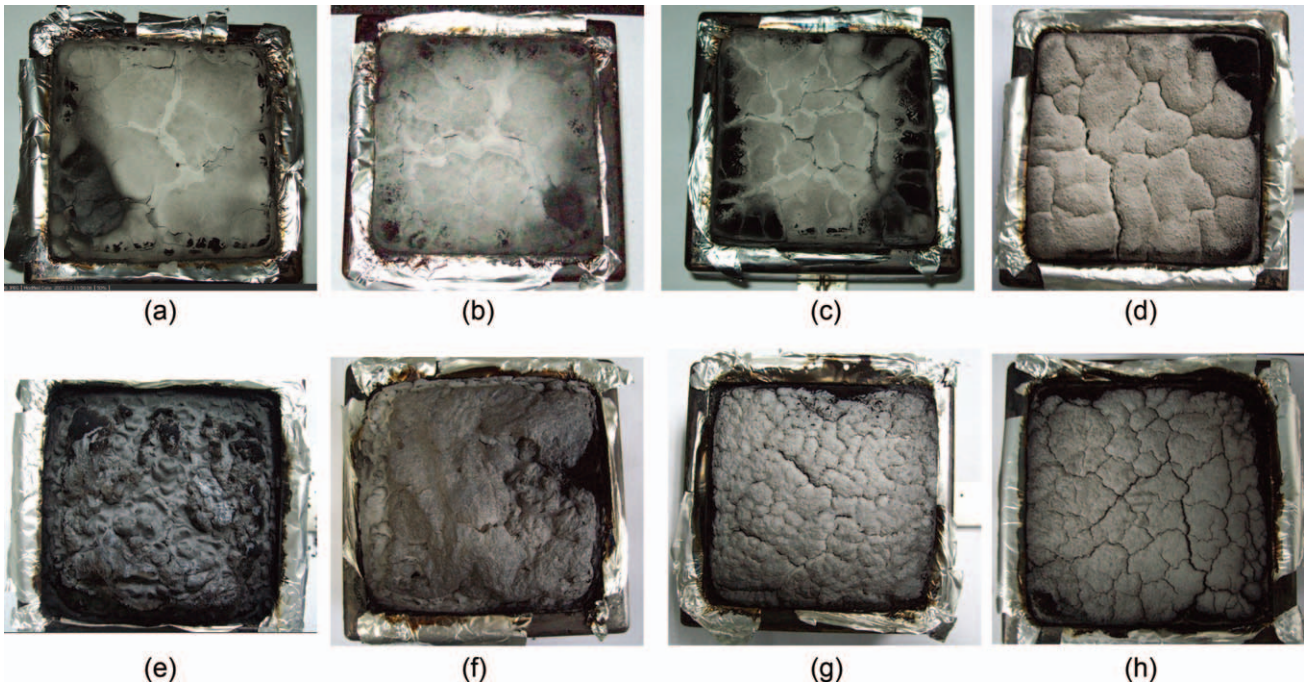

Figure 4. Morphologies of the residues produced from the composites after cone calorimeter test. [Color figure can be viewed in the online issue, which is available at wileyonlinelibrary.com.]

are shown in Figure 3 and the cone calorimeter test data are listed in Table II. Both mean HRR and pHRR of the composites change significantly during the combustion test in comparison with the matrix. The HRRs of POE and POE-*g*-MAH matrix increase more rapidly than those of the composites, reaching peaks of 1374 kW/m^2 at 265 s and 1571 kW/m^2 at 301 s, respectively. For the composites, the time at HRR peak is retarded and the peak values are decreased with the addition of the OMMT. The suggested mechanism by which clay nanocomposites function involves the formation of a char that serves as a potential barrier to both mass and energy transport.[22] A ceramic-like layer is formed at the surface of the material in which the efficiency is dependent on the homogeneity of the forming layer.[23]

The PHRR of POE and POE-*g*-MAH with 5 wt % OMMT display 31% and 62% reductions, respectively, compared with their matrix. The results reveal that a good dispersion of OMMT gives rise to a better performance of POE-*g*-MAH/OMMT nanocomposites compared with POE/OMMT microcomposites. The morphologies of the residues produced from the composites after cone calorimeter test are shown in Figure 4. POE/OMMT (5 wt %) microcomposites and POE-*g*-MAH/OMMT (5 wt %) nanocomposites display different combustion behavior due to the different dispersion of OMMT layers. Zanetti and Luigi[24] studied that, in the case of the microcomposite, the clay layers alone are not able to product a continuous protective stratum. The better effect is due to the barrier effect of the exfoliated nanostructure in the nanocomposite. As shown in Figure 4(a, e), the residue of POE/OMMT (5 wt %) displays thin and nonuniform char but relatively thick, dense char formed in POE-*g*-MAH/OMMT (5 wt %) one. The improvement of flame retardancy of POE-*g*-MAH/OMMT nanocomposites can be attributed to the good barrier properties and protective effect of organoclay.

From Table II and Figure 4, a clear difference in residue yield and char morphology could be observed with the addition of the OMMT. For both series of the composites, the residue yield increases and with less OMMT produce significant char, and

Table III. Cone Calorimeter Test Data of Composites

	Mean SEA (m^2/kg)		Mean EHC (MJ/kg)		Mean CO yield (kg/kg)	
OMMT (wt %)	POE/OMMT	POE-*g*-MAH/OMMT	POE/OMMT	POE-*g*-MAH/OMMT	POE/OMMT	POE-*g*-MAH/OMMT
0	334	334	47	42	0.0348	0.0318
5	386	468	47	43	0.0376	0.0356
15	468	493	46	43	0.0362	0.0406
25	444	445	46	44	0.0366	0.0394
35	416	399	46	44	0.0373	0.0395

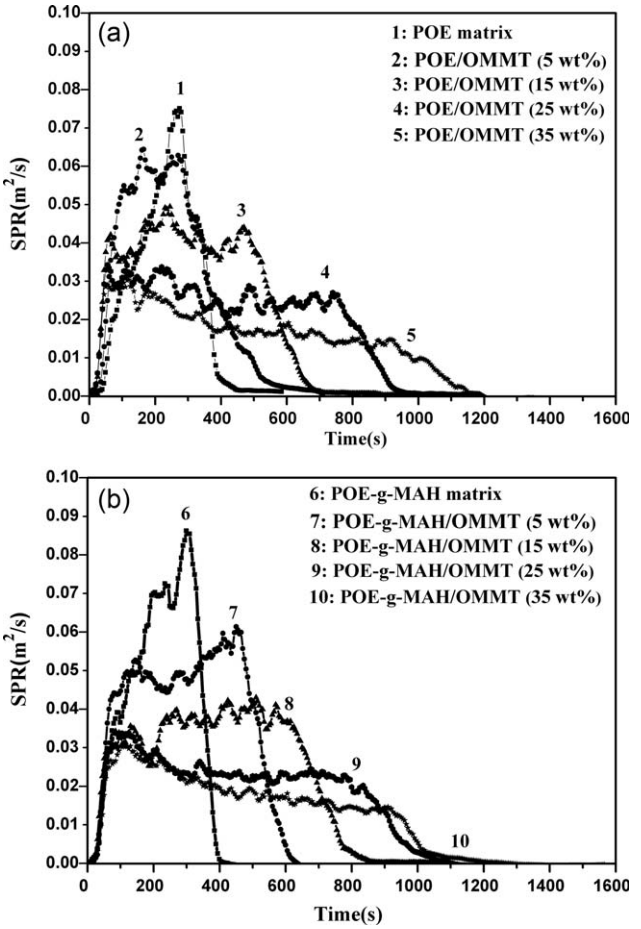

Figure 5. SPR curves of POE/OMMT (a) and POE-*g*-MAH/OMMT (b) composites.

the char is surface revealed with few fine cracks. However, the composite with more OMMT form a consolidated char with more cracks. That is the reason why incorporation of OMMT (15 wt %, 25 wt %, 35 wt %) into matrix leads to an additional but limited decrease in pHRR. At the same content of OMMT, the residue yield of POE-*g*-MAH/OMMT nanocomposite is more and the char is dense with less cracks than that of POE/OMMT microcomposite.

The SEA, EHC, and CO yield data were shown in Table III. EHC and CO yield are almost unchanged, suggesting that the source of the improved flammability properties of these materials is due to differences in condensed-phase decomposition processes and not in the gas-phase effect.

However, a somewhat difference is found for the SEA between the two series of composites. The SEA indicates the average value of the smoke evolved per mass unit of volatiles degraded from the sample on burning. It is generally supposed that the volatile combustible products formed from the pyrolysis of polymer resin tend to leave the sample instantaneously. By leaving the polymer, these products cause the silicate to migrate to the sample surface and the clay layers become the dominant material, which might derive from the barrier effect for the diffusion of the volatile decomposition products to the gas phase and oxygen from the gas phase to the polymer.[25,26] The released volatiles can not be burn enough due to the lack of exchange of oxygen leading to the increase of mean SEA. POE-*g*-MAH/OMT nanocomposite has better barrier properties and protective effect of organoclay, resulting in a higher mean SEA than that of POE/OMMT microcomposite at the same content of OMMT.

In this article, SPR indicates the danger of smoke production instead of SEA and is described as Formula (1). The SPR curves are shown in Figure 5.

$$\mathrm{SPR} = \mathrm{MLR} \times \mathrm{SEA}$$

In Figure 5, the SPR of both the POE/OMMT and POE-*g*-MAH/OMMT composites are appreciably lower compared with their matrix, respectively. Thus, the danger of smoke production is reduced for the two series of composites.

CONCLUSION

TEM micrographs show agglomerated structure of OMMT within POE matrix but intercalated/exfoliated structures throughout POE-*g*-MAH matrix. TGA results show that the thermal stability of POE-*g*-MAH/OMMT nanocomposite is better than that of POE/OMMT microcomposite and the better thermal stability is not due to the higher thermal stability of POE-*g*-MAH matrix but because of the strong effect of the better dispersion of OMMT. Cone calorimeter test results show that TTI for both series of composites are shorter compared with their matrix, respectively. Both mean HRR and pHRR of the composites change significantly during the combustion tests in comparison with the matrix. EHC and CO yield are almost unchanged, suggesting that the source of the improved flammability properties of these materials is due to differences in condensed-phase decomposition processes and not in the gas-phase effect. POE-*g*-MAH/OMMT nanocomposites have better improvement in flame retardancy than POE/OMMT microcomposites because of the different dispersion of OMMT layer. The better improvement is attributed to the barrier effect of the exfoliated nanostructure in the nanocomposite.

ACKNOWLEDGMENTS

This work were supported by National Natural Science Foundation of China (20964001), National Natural Science Foundation of China (50863001), Project 973 (2011CB612313), and Science and Technology Developing Project of Guizhou province [contract/grant number: (2009)3010].

REFERENCES

1. Ganesh, L.; Quentin, L.; Riko, O. J. *Mater. Sci.* **2008,** *43*, 2555.
2. Jeffrey, W. G.; Richard, H. H. J.; John, R. S. *Polym. Adv. Technol.* **2006,** *17*, 263.
3. Liao, H. T.; Chin, S. W. *Appl. Polym. Sci.* **2005,** *97*, 397.
4. Jeffrey, W. G. *Appl. Clay Sci.* **1999,** *15*, 31.

5. Huaili, Q.; Quansheng, S.; Shimin, Z. *Polymer* **2003,** *44*, 7533.
6. Zanetti, M.; Kashiwagi, T.; Falqui, L.; Camino, G. *Chem. Mater.* **2002,** *14*, 881.
7. Jeffrey, W. G.; Catheryn, L. J.; Alexander, B. M. *Chem. Mater.* **2000,** *12*, 1866.
8. Fabienne, S.; Serge, B.; Charafeddine, J. *Polym. Degrad. Stab.* **2008,** *93*, 2019.
9. Zanetti, M.; Pierangiola, B.; Luigi, C. *Polym. Degrad. Stab.* **2004,** *85*, 657.
10. Bourbigot, S.; Gilman, J. W.; Wilkie, C.A. K. *Polym. Degrad. Stab.* **2004,** *84*, 83.
11. Young, W. C.; Dongsuk, L.; Bae, S. Y. *Polym. Int.* **2006,** *55*, 84.
12. Hrissopoulou, K.; Anastasiadis, S. H. *Eur. Polym. J.* **2010,** *09*, 1.
13. Yibing, C.; Fenglin, H.; Xin, Xia. *JMEPEG* **2010,** *19*, 171.
14. Chungui, Z.; Huaili, Q.; Fangling, G. *Polym. Degrad. Stab.* **2005,** *87*, 183.
15. Zanetti, M.; Camino, G.; Thomann, R. *Polymer* **2001,** *42*, 4501.
16. Xie, W.; Gao, Z.; Pan, W. P.; Hunter, D.; Singh, A.; Vaia, R. *Chem. Mater.* **2001,** *13*, 2979.
17. Qin, H.; Zhang, Z.; Feng, M.; Gong, F.; Zhang, S.; Yang, M. J. *Polym. Sci. Part B: Polym. Phys.* **2004,** *42*, 3006.
18. Qin, H.; Zhang, Z.; Feng, M.; Gong, F.; Yang, M.; Shu, Z. *Polym. Degrad. Stab.* **2004,** *85*, 807.
19. Zanetti, M.; Camino, G.; Reichert, P. *Macromol. Rapid Commun.* **2001,** *22*, 176.
20. Haiyun, M.; Zhongbin, X.; Lifang, T. *Polym. Degrad. Stab.* **2006,** *91*, 2951.
21. Shaofeng, W.; Yuan, H.; Ruowen, Z. *Appl. Clay Sci.* **2004,** *25*, 53.
22. Zhu, J.; Morgan, A. B.; Lamelas, F. J.; Wilkie, C. A. *Chem. Mater.* **2001,** *13*, 3774.
23. Kashiwagi, T.; Richard, H. H. J.; Zhang, X.; Briber, R. M.; Cipriano, B. H. ;Raghavan, S. R. *Polymer* **2004,** *45*, 881.
24. Zanetti, M.; Luigi, C. *Polymer* **2004,** *45*, 4367.
25. Tsu, H. C.; Wenjeng, G.; Kuo, C. C. *J. Polym. Res.* **2004,** *11*, 169.
26. Haiyun, M.; Lifang, T.; Zhongbin, X.; Zhengping, F. *Polym. Degrad. Stab.* **2007,** *92*, 1439.